

IV. NUCLEAR MAGNETIC RESONANCE AND HYPERFINE STRUCTURE

Prof. F. Bitter
Prof. J. S. Waugh
Dr. L. C. Bradley III
Dr. H. H. Stroke
Dr. J. F. Waymouth
T. Fohl
R. L. Fork
J. V. Gaven, Jr.

W. D. Halverson
E. R. Hegblom
Ilana Levitan
F. A. Liégeois
J. D. Macomber
F. Mannis
I. G. McWilliams
P. G. Mennitt

S. R. Miller
H. C. Praddaude
O. Redi
C. J. Schuler, Jr.
R. W. Simon
W. W. Smith
W. J. Tomlinson III
W. T. Walter

A. CORKSCREW INSTABILITY

A very convenient demonstration of a corkscrew instability in a magnetic field is described by Elenbaas¹ in his book on high-pressure mercury arcs. We have tried this with the results shown in Figs. IV-1 and IV-2. Several commercial high-pressure

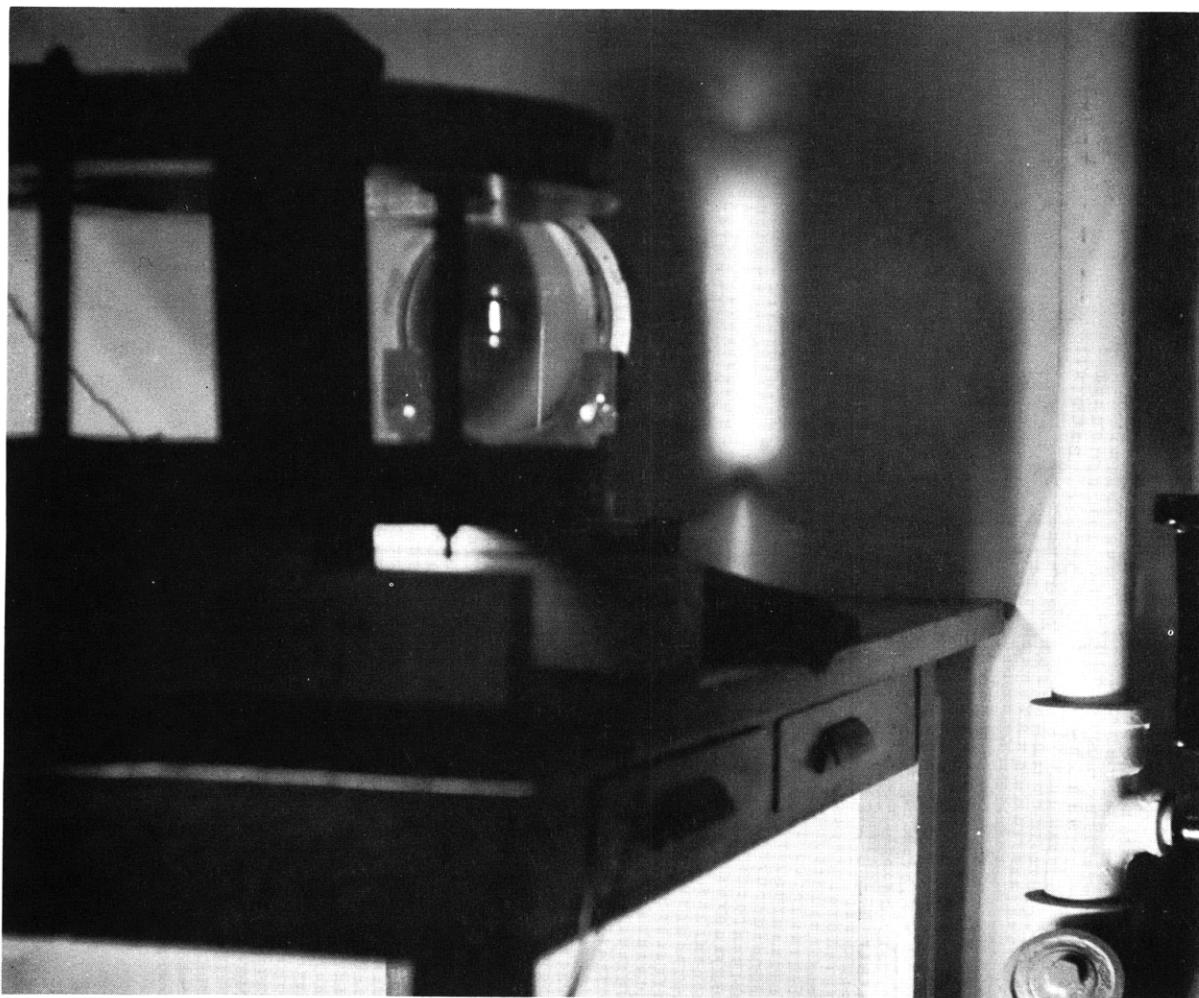


Fig. IV-1. Apparatus for exhibiting a very bright high-pressure mercury arc. The image on the wall is for the arc in zero magnetic field.

(IV. NUCLEAR MAGNETIC RESONANCE)

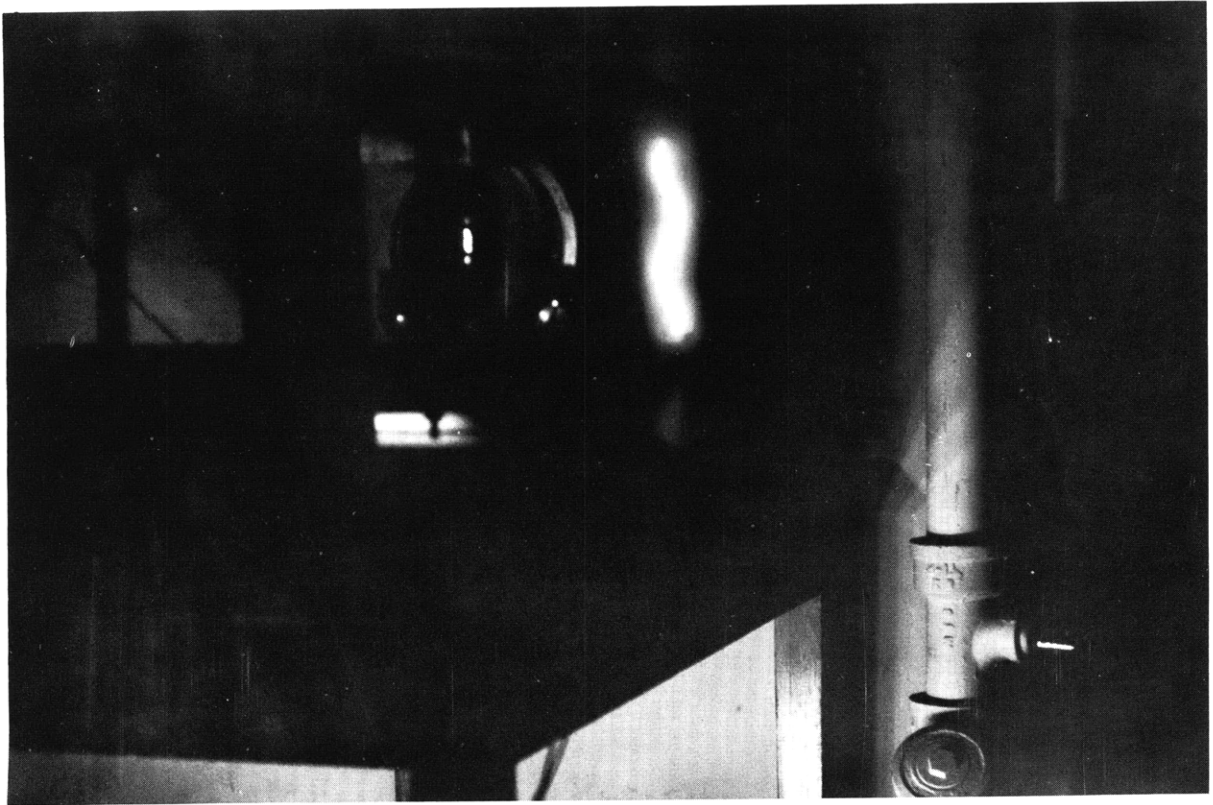


Fig. IV-2. Spiral shape assumed by the arc in the presence of an axial magnetic field of ~ 50 gauss.

mercury arcs have been used. In Fig. IV-1 the arc is inside of a metal chimney along the axis of a pair of Helmholtz coils. A large lens focuses an image of the arc on a wall. As the field is turned on, the arc shows a tendency to spiral. Around 50 gauss it is usually steady, as in Fig. IV-2, but at higher fields the spiral rotates faster and faster. Under certain conditions the spiral may bob up and down without rotating. The details of the motion seem to be associated with conditions at the electrodes.

F. Bitter

References

1. W. Elenbaas, The High Pressure Mercury Vapor Discharge (North Holland Publishing Company, Amsterdam, 1951). (Distributed by Interscience Publications, Inc., New York.)

B. HIGH-POWER SOLENOID ELECTROMAGNET

A high-power water-cooled solenoid electromagnet, designed by Bruce Montgomery of the National Magnet Laboratory, has been built and put into operation (Fig. IV-3).

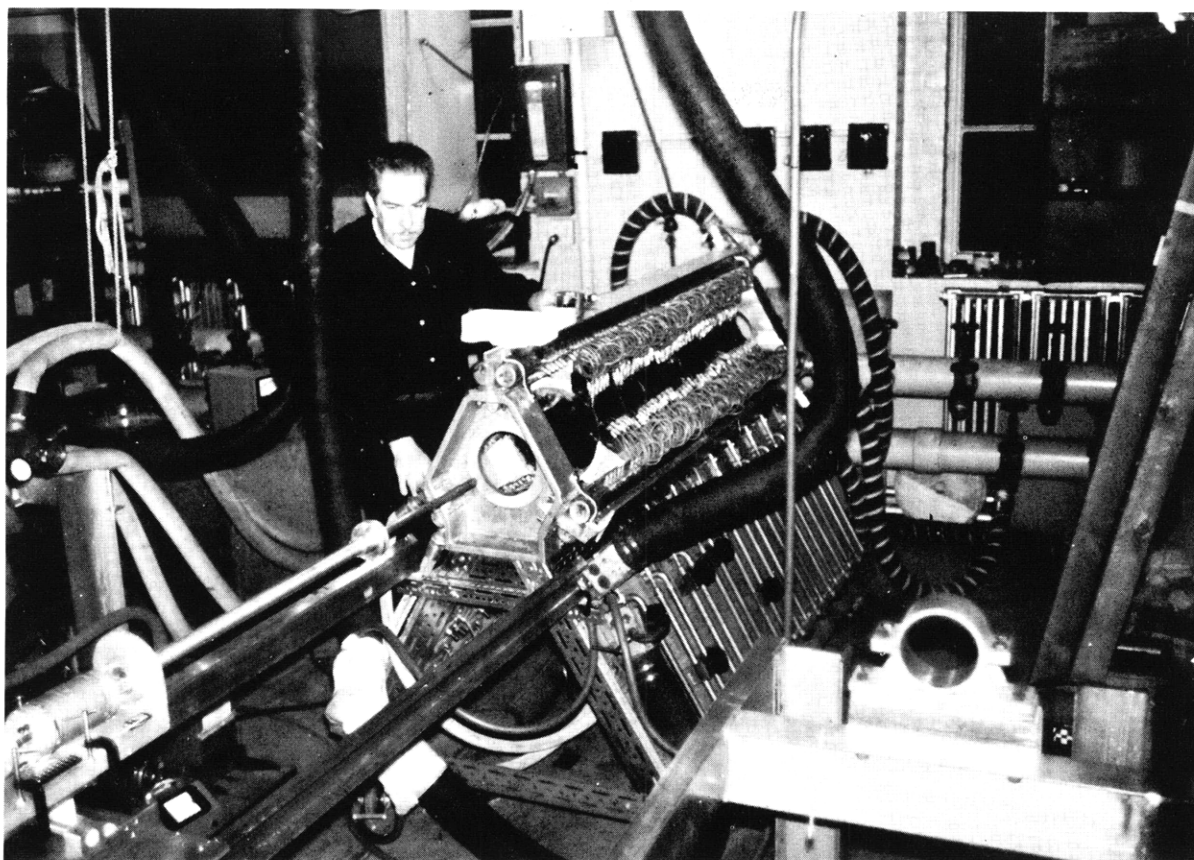


Fig. IV-3. Water-cooled coils used to produce an axial magnetic field in the positive column of various types of gas discharge.

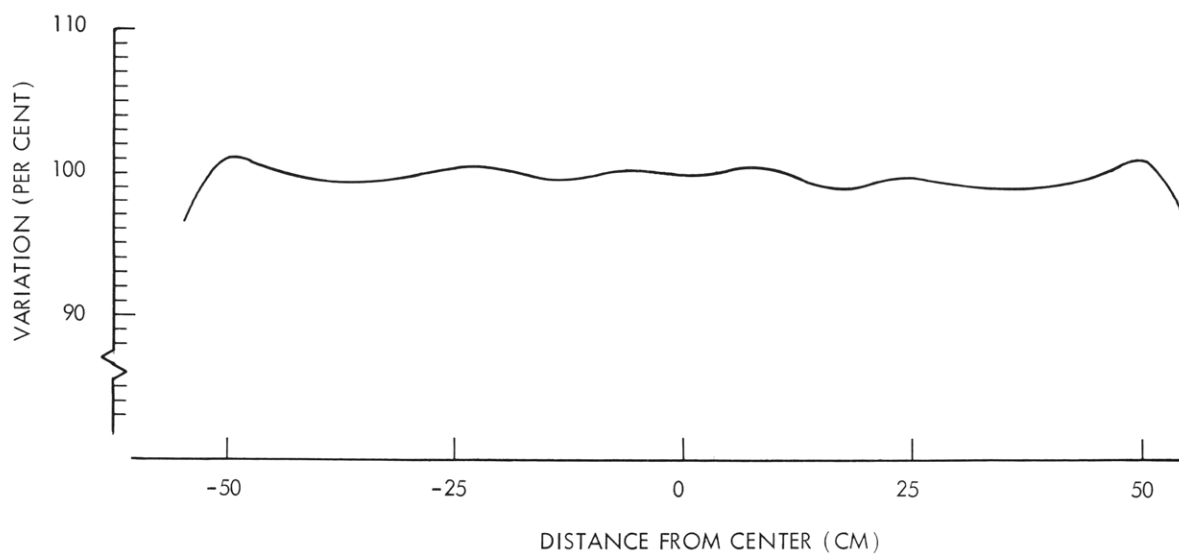


Fig. IV-4. Solenoid electromagnet field variation vs axial position. Field at center position = 100 per cent. Field/current ratio = 3.38 gauss/ampere.

(IV. NUCLEAR MAGNETIC RESONANCE)

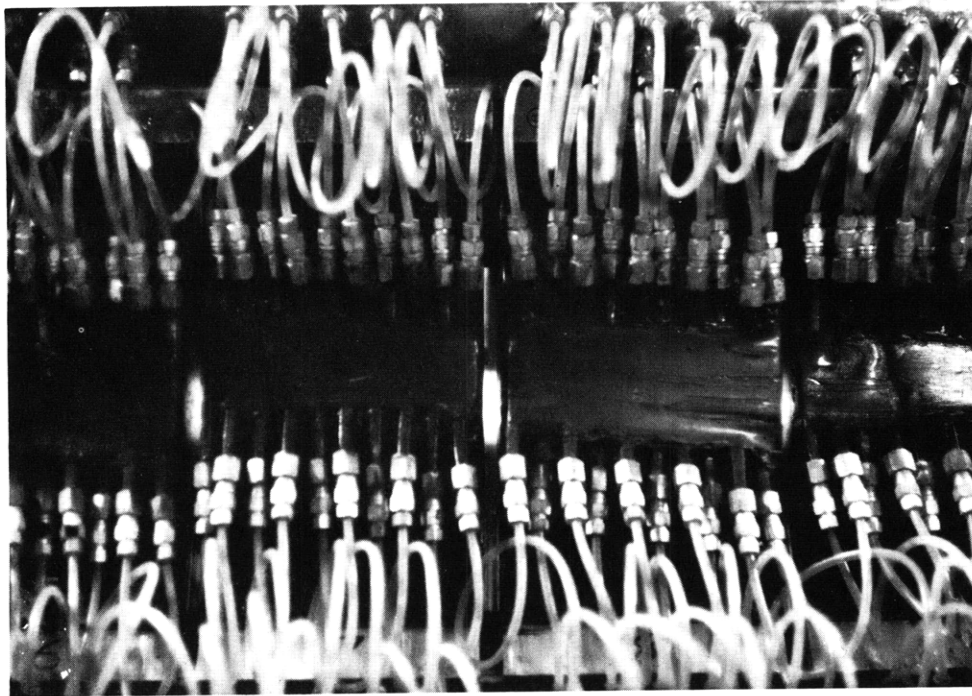


Fig. IV-5. Photograph of a plasma as seen between adjacent coils.

The magnet that is now being operated consists of eight coils that produce a homogeneous magnetic field in a region approximately 1 meter long and 10 cm in diameter. Two more coils are available to extend the length of the field approximately 30 cm.

The electromagnet has been successfully operated to fields up to 17,000 gauss, and when new power supplies are available the field may be doubled. The present maximum operating level is 5000 amps, 180 volts (900 kilowatts).

Figure IV-4 shows the measured variation of the magnetic field along the axis of the solenoid. The field is homogeneous within less than 2 per cent over a 104-cm axial traverse. Within the magnet the field varies less than 0.5 per cent over a 5-cm radius from the solenoid axis. Figure IV-3 shows the ten 20 kilowatt rheostats used to trim each coil for maximum homogeneity.

The solenoid will be used for studies of electrical discharges in gases under the influence of axial magnetic fields. Figure IV-5 shows the plasma of a low-pressure argon discharge as viewed through the gap between two coils.

F. Bitter, W. D. Halverson

C. QUADRUPOLE MAGNET AND TRANSVERSE-FIELD MAGNET FOR PLASMA STUDIES

A quadrupole magnet, 2 feet long and of 2 inches aperture, and a "shoe box" magnet, 2 feet long, with a 2-inch gap for studying the interaction of fields of various

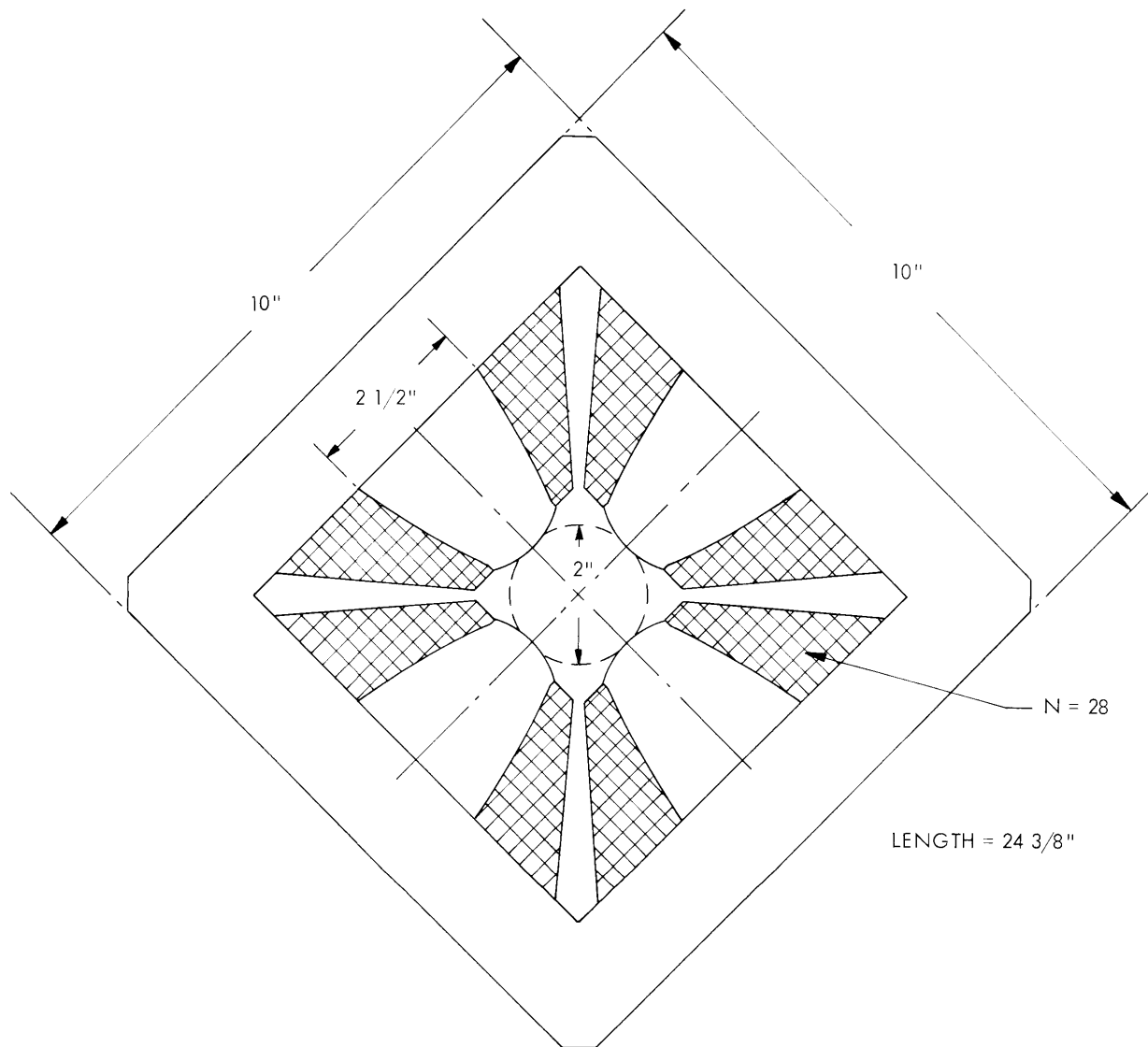


Fig. IV-6. Configuration of the quadrupole magnet.

(IV. NUCLEAR MAGNETIC RESONANCE)

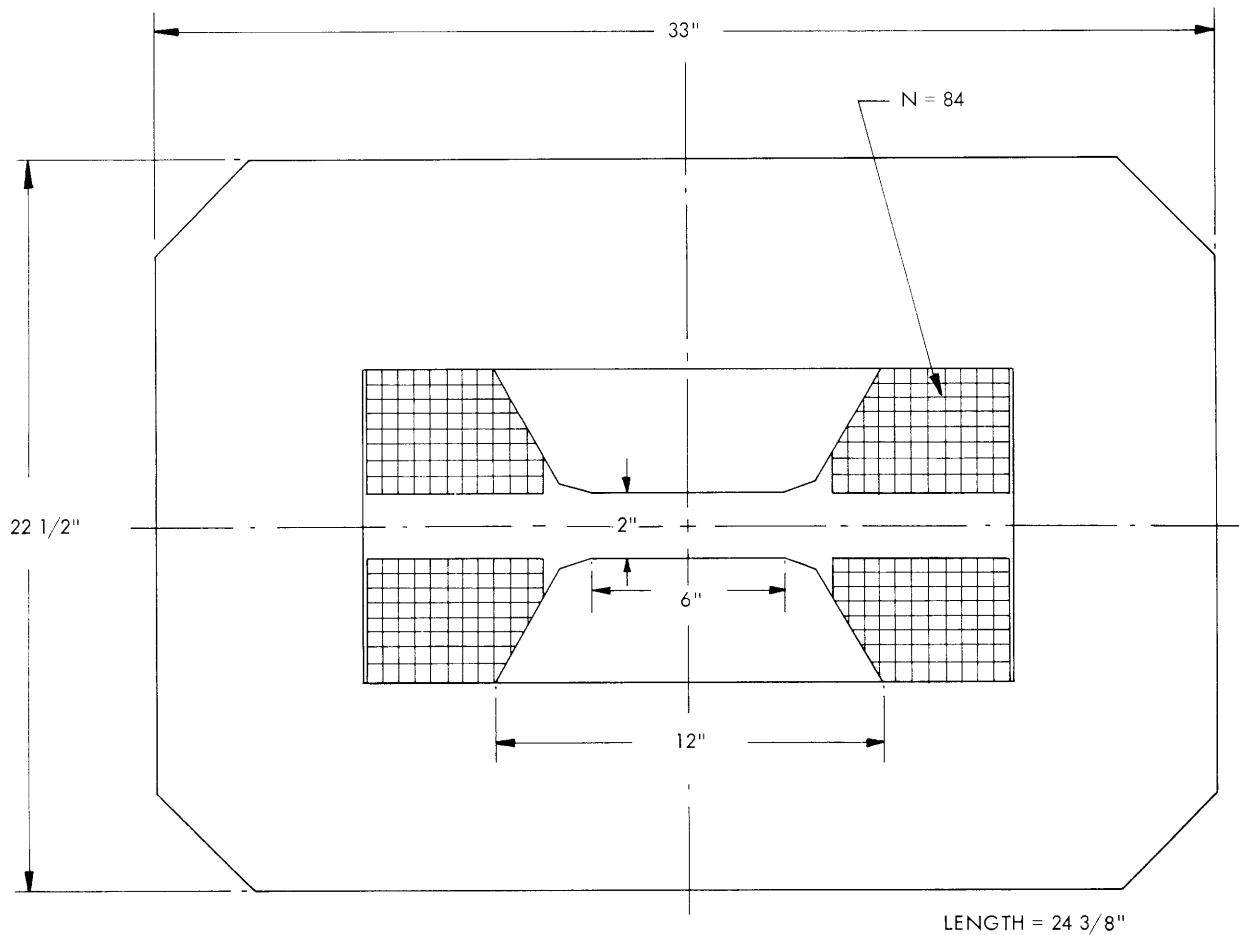


Fig. IV-7. Configuration of the transverse field magnet.

configurations with plasmas, have recently been completed and put into operation. They were designed by H. Brechna of the National Magnet Laboratory. Sketches of the configuration of these magnets and photographs of the actual magnets in operation are shown in Figs. IV-6 to IV-9. Each magnet has three narrow slots through which the positive column of the discharge may be viewed directly. The specifications and calibrations of these magnets are:

Quadrupole magnet

650 lbs

Maximum current, 700 amps

Maximum voltage, 80 volts

Turns per pole, 28 (total 112)

Observed gradient at 400 amps, slightly more than 10 kg/inch

Calculated gradient at 700 amps, slightly more than 14 kg/inch

The field is constant within 2 per cent 1 inch from the center over ~18 inches

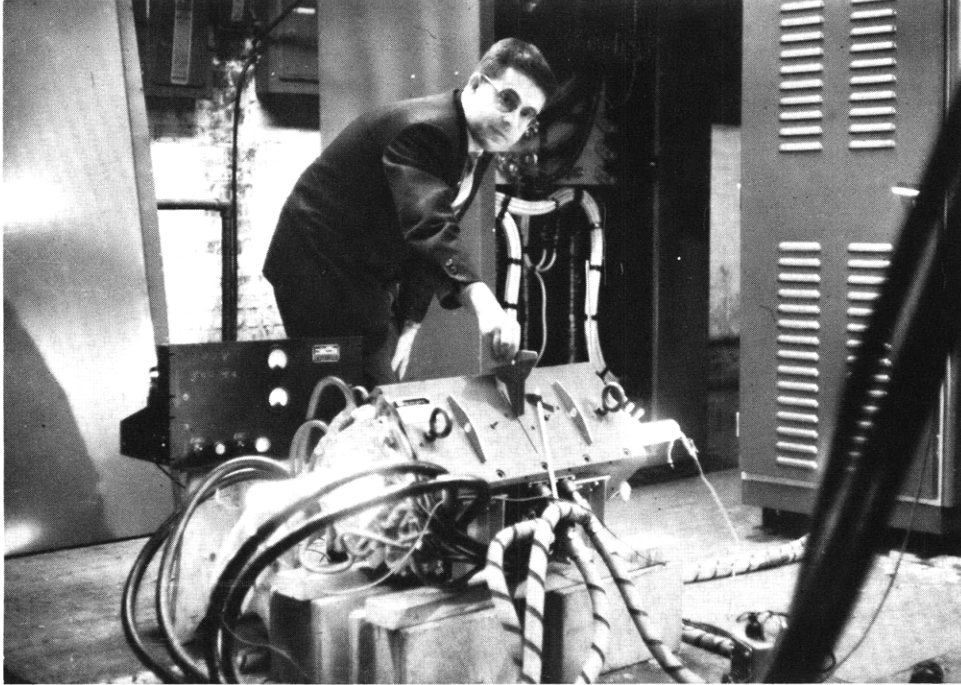


Fig. IV-8. The quadrupole magnet.



Fig. IV-9. The transverse-field magnet.

(IV. NUCLEAR MAGNETIC RESONANCE)

at 300 amps, and over ~12 inches at 400 amps.

Transverse-field magnet

5500 lbs

Maximum current, 700 amps

Maximum voltage, 80 volts

Turns per pole, 84 (total 168)

At the center, the field is 17,000 gauss at 410 amps and is uniform to better than 1 per cent along 22 inches of the central axis. The calculated magnetic field at 700 amps is 21,000 gauss.

F. Bitter, B. Afshartous

D. HYPERFINE STRUCTURE AND ISOTOPE SHIFTS IN Hg^{195} , Hg^{195*} , Hg^{194} , AND Hg^{193*}

The work on Hg^{195} , Hg^{195*} , and Hg^{194} described in Quarterly Progress Report No. 65 (page 39) has been refined, and extended to Hg^{193*} . The following results have been obtained:

$$\text{Hg}^{195}: I = 1/2$$

$$\mu = +0.5347 \pm 0.0044 \text{ nm.}$$

$$\text{Hg}^{195*}: I = 13/2 \pm 0.60$$

$$\mu = -1.0390 \pm 0.0058 \text{ nm}$$

$$Q = (1.5 \pm 0.6) \times 10^{-24} \text{ cm}^2.$$

Isotope shifts (2537 Å line):

$$\text{Hg}^{194} - \text{Hg}^{198} = 0.308 \pm 0.015 \text{ cm}^{-1}$$

$$\text{Hg}^{195} - \text{Hg}^{198} = 0.210 \pm 0.015 \text{ cm}^{-1}$$

$$\text{Hg}^{195*} - \text{Hg}^{198} = 0.215 \pm 0.015 \text{ cm}^{-1}.$$

The magnetic moment values do not include the diamagnetic correction. The indicated errors are two standard deviations, and represent only random errors. The work on Hg^{193*} has not progressed sufficiently so that we can give definite values, but it appears that the spin is probably 13/2, and the magnetic moment within 1 or 2 per cent of the value for the Hg^{195*} moment.

The isotope-shift data have shown interesting systematics, and perhaps provide a clue to the problem of odd-even staggering effects in isotope shifts. These conclusions have been written up and submitted for publication.

Further work will be directed toward obtaining results for Hg^{193} and Hg^{193*} , and improving the isotope-shift data for the other isotopes. A study will be undertaken to determine the reason for the nonappearance of Hg^{193} in our last run, so that future runs may be designed to maximize the relative amount of

(IV. NUCLEAR MAGNETIC RESONANCE)

Hg¹⁹³ in our light sources. Pictures are being taken of the older light sources in order to plot the decay of Hg¹⁹⁴, and obtain a direct measurement of its halflife.

W. J. Tomlinson III, H. H. Stroke

E. A PERTURBATION SOLUTION OF THE EQUATION OF MOTION FOR THE DENSITY MATRIX

A solution of the Laplace transform of the equation of motion for the density matrix has been obtained in terms of a resolventlike operator. A suitable expansion of the resolvent operator has been obtained, which is equivalent, essentially, to performing explicitly a large number of partial summations in the standard expansion. The final result can be written in a very convenient form, since it exhibits explicitly, even in the lowest order, properties of the system that is under study, such as resonances and relaxation times, which are of the greatest interest.

A few simple cases have been considered and the formalism will be applied to some problems that are pertinent to our experimental work.

H. C. Praddaude

F. LOCAL ENERGY BALANCE OF THE ELECTRON GAS IN A SPHERICAL PLASMA

Previous reports^{1, 2} have described the behavior of a dc discharge in a mixture of mercury vapor and rare gas in a spherical tube. It has been shown that when the anode is very near the cathode, at the center of the tube, a plasma is generated which has spherical symmetry. Heat conduction, radiation diffusion, and particle diffusion all take place, transferring plasma and energy from the center to the walls. A discussion of the diffusion of ions and electrons was given in the Quarterly Progress Report No. 65. In this report the energy balance of a small volume of electron gas, not near the center nor the walls, is considered.

The situation in the volume is that the electrons are far from equilibrium with the gas atoms and ions. The electron gas temperature is approximately 4000°K or 5000°K, while the gas of ions and atoms is at room temperature. The electron gas can be cooled by elastic and inelastic collisions with the atoms, and can be heated by electric fields and by collisions with excited atoms. Also, heat is conducted into and out of the volume.

The conditions for which this discussion is intended are: the rare gas is helium at a pressure of approximately 1 mm Hg; the electron density is 10^{16} electrons per cubic meter; the electron temperature is less than 6000°K; and the mercury vapor pressure is 1 micron. Under these conditions, we can say that inelastic collision energy losses are 1 per cent, or less, of elastic collision losses; the mean-free path of the electrons

(IV. NUCLEAR MAGNETIC RESONANCE)

is determined by collisions with helium and is constant; only mercury atoms are excited; and heating resulting from electric fields is negligible.

Since the mean-free path in helium is nearly a constant function of energy, for such cool electrons the rate of energy loss by elastic collisions may be calculated simply by

$$\begin{aligned} W_L &= \frac{4\sqrt{m_e}}{M_g \sqrt{\pi}} (2kT_e)^{3/2} \sigma_c N_a \\ &= 2.42 \cdot 10^{-44} N_a T_e^{3/2} \text{ watts/electron} \end{aligned} \quad (1)$$

where W_L is the energy loss rate per electron in watts, T_e is the electron temperature in °K, N_a is the density of helium atoms in m^{-3} , σ_c is the cross section for electron collisions with helium in m^2 . Typically, the energy loss is approximately 300 watts per cubic meter.

The resonance radiation emitted by the mercury atoms that are excited in the region of the cathode excites atoms in the outer regions of the plasma. The radiation consists of the mercury 2537 Å and 1849 Å lines. The other lines of mercury arise from transitions that terminate on excited states. Atoms in these states are sufficiently rare in the outer regions of the discharge so that these photons pass through the gas without absorption. Only in the region of the cathode are electrons energetic enough to appreciably excite the atoms from the ground level to the 6^1P_1 and 6^3P_1 levels that give rise to the 1849 Å and 2537 Å lines, respectively. Since the energy distribution is unknown in this region, the relative importance of the two lines is not calculable.

As the resonance radiation diffuses outward, it causes excited atoms to occur in the outer regions of the plasma. Electrons colliding with these excited atoms can de-excite them and gain energy from them. These are called "superelastic collisions." Meta-stable atoms also diffuse outward and can give rise to the same effect, but in this geometry they are neglected because of their slow diffusion rate.³ In this report only the superelastic collision rates are calculated, and the details of the diffusion of resonance radiation are ignored.

The cross section for electronic de-excitation can be calculated from the excitation function by the Klein-Rosseland relation³

$$Q_{21}(V') = \frac{g_1}{g_2} \frac{V}{V - V_e} Q_{12}(V), \quad (2)$$

where

$Q_{21}(V')$ is the cross section for quenching state 2 to state 1;

$Q_{12}(V)$ is the cross section for electron excitation of state 2;

g_1 and g_2 are the statistical weights of the two states;

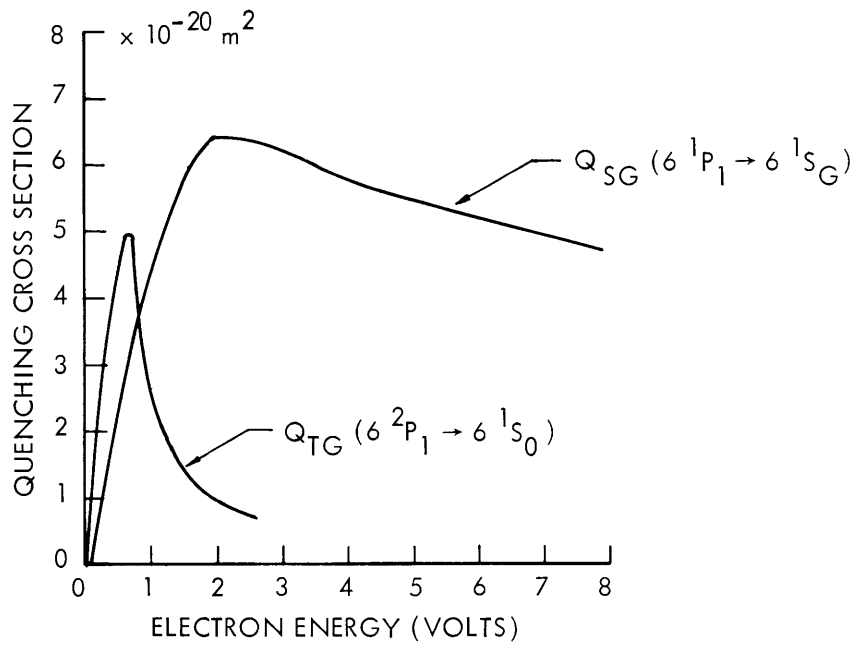


Fig. IV-10. Cross sections for electronic de-excitation of the resonance levels of mercury.

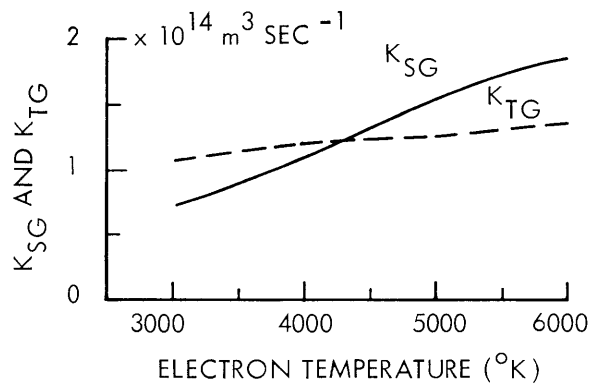


Fig. IV-11. Quenching rate per electron per excited atom for the singlet resonant state, K_{SG} , and triplet resonant state, K_{TG} , of mercury.

(IV. NUCLEAR MAGNETIC RESONANCE)

V_e is the excitation potential;

V is the voltage for the excitation curve; and

V' is the voltage for the de-excitation curve.

The cross sections for quenching the singlet state to ground, Q_{SG} , and for quenching the triplet state to ground, Q_{TG} , are plotted in Fig. IV-10.

The de-excitation rate is obtained by multiplying the cross section by the energy distribution function and integrating over all energies. Following the procedure of Bitter and Waymouth,⁴ we evaluate the function given in relation (3) graphically.

$$K = 2\sqrt{\frac{2kT_e}{\pi m_e}} \int_0^\infty \epsilon Q(V) e^{-\epsilon} d\epsilon. \quad (3)$$

Here, K multiplied by the number of electrons and excited atoms per unit volume is the number of quenchings per second per unit volume; $\epsilon = \frac{eV}{kT_e}$, with eV the energy and T_e the electron temperature; and $Q(V)$ is the cross section as a function of V . The values of K_{TG} and K_{SG} thus obtained are plotted as a function of electron temperature in Fig. IV-11.

The energy gain to the electron gas from each superelastic collision is eV_T from the triplet state, and eV_S from the singlet state ($V_S = 6.7$ volts and $V_T = 4.9$ volts). The energy transferred from the excited atoms to the electrons per second per unit volume, W_G , is given by

$$W_G = N_T N_e K_{TG} eV_T + N_S N_e K_{SG} eV_S \text{ watts/m}^3, \quad (4)$$

where N_T and N_S are densities of atoms excited to the triplet and singlet states, and N_e is the density of electrons.

Thus a region in which W_G exceeds W_L is a source of heat to the electron cloud, while a region in which W_L is greater than W_G is a sink of heat.

In order to determine the density of radiation and excited states, several modifications have been made to the probes in the spherical tube described in the previous reports.^{1, 2} A phosphor that emits a known intensity of visible light for a given intensity of incident 2537 Å and 1849 Å radiation has been applied to the glass sheath of the probes. Part of the phosphor is shielded with Vycor which excludes 1849 Å light, but not 2537 Å light. By measuring the intensity of the visible light emitted by the phosphors by means of a photomultiplier and suitable filters, the density of 2537 Å and 1849 Å radiation in the region of the probe can be determined. In this way, the radial distribution of radiation density is to be determined.

To measure the density of excited states directly, an absorption experiment is planned. A beam of light whose frequency is characteristic of a transition between the resonance excited level and a still higher level is passed through the plasma. The

(IV. NUCLEAR MAGNETIC RESONANCE)

absorption of the beam will be proportional to the number of excited atoms along its path. A small mirror is attached to the end of a movable probe, and the beam will enter and be reflected out in a radial direction. By measuring the absorption of the beam at various radial positions of the mirror, a determination of the distribution of excited states should be possible.

T. Fohl

References

1. T. Fohl, Study of d-c discharges in a large spherical vessel, Quarterly Progress Report No. 64, Research Laboratory of Electronics, M.I.T., January 15, 1962, pp. 40-42.
2. T. Fohl, D-C discharge in the large spherical lamp, Quarterly Progress Report No. 65, op. cit., April 15, 1962, pp. 41-43.
3. C. Kenty, J. Appl. Phys. 21, 1309-1312 (1950).
4. F. Bitter and J. F. Waymouth, Sylvania Electric Corporation Report (unpublished).

